Molecular Orientation of Extruded PET/LCP Blend Films. II. X-Ray Pole Figures

Marcia C. Branciforti, Lucineide B. Silva, Rogerio Machado, Rosario E. S. Bretas

Department of Materials Engineering, Federal University of São Carlos Rod. Washington Luis, CEP13565-905, São Carlos, SP, Brazil

Received 7 February 2007; accepted 22 April 2007
DOI 10.1002/app.26780
Published online 9 August 2007 in Wiley InterScience (www.interscience.wiley.com).

ABSTRACT: The crystalline uniaxial molecular orientation of two liquid crystalline polymers (LCPs), Vectra® A950, and Rodrun® LC5000, blended with poly(ethylene terephthalate) (PET) was obtained from wide angle X-ray pole figures. The blends films were produced by extrusion using a twin screw extruder with a slit die. The molecular orientation was evaluated along the transverse section of the films and as a function of the blends composition. The influence of a compatibilizer agent on the LCPs orientation was also analyzed. It was found that the orientation of both LCPs in the pure LCP films was high, highest in the draw direction but variable along the transverse section of the extruded films; in this last case, it was higher at the position where the shear rate was maximum. However, a drastic orientation decrease in both LCP's phases was observed in the films made of PET/LCPs blends. The maximum orientation effects were observed for the blend with 5 wt % of LCP content and also at the position where the shear rate was the highest. The Vectra® A950 LCP, as a pure material and in the blend with PET, orient more effectively than the Rodrun® LC5000 LCP in the films produced at the same processing conditions. The results showed that the use of a compatibilizer agent decreased the LCP orientation and were in accordance with previous studies using polarized infrared spectroscopy. © 2007 Wiley Periodicals, Inc. J Appl Polym Sci 106: 2955–2962, 2007

Key words: LCP; orientation; pole figure; PET; blends

INTRODUCTION

Characterization of molecular orientation in blends of thermoplastics and liquid crystalline polymers (LCP) is important since most of the rheological, physical, and mechanical properties of these blends depend on the extent of LCP orientation.[1–13] It is also known that the orientation is influenced by a variety of parameters, such as LCP content, processing and thermal histories, and the chemical structure of the blend components. Rigid molecules of LCPs with long relaxation times usually exhibit a low viscosity in the mesophase and are capable of orientation parallel to the flow direction, which is almost always maintained after solidification. Well-oriented LCP fibrils would provide effective reinforcement to the thermoplastic polymer. Morphological studies[14–18] indicated that the as-blended, drop-like dispersion of the LCP phase could be deformed into long oriented fibers during processing. The possibility of orientation is due to the rigid chemical structure of the LCP, which can gives rise in the solid state to fibrillar structures with high stiffness and strength that are called ''*in-situ*'' composites. There are many factors affecting the mechanical properties of these ''*in situ*'' composites, which are generally limited by the intrinsic immiscibility of the blend components. For this reason, compatibilization by different methods is often used to improve the interfacial interactions, mostly using ethylene copolymers with acrylic.[18–22] Analogous compatibilizer was used in this work.

Many reports described studies of blends of PET with LCP obtained by different processing conditions.[12,13,18,23–36] In general, these studies demonstrated that the mechanical properties of the blends are significantly affected by the mode of dispersion, shape, and orientation of the LCP and the interfacial interactions between the two phases. In some cases, significant improvement in strength and stiffness are found. In fibers of PET/LCP blends prepared by melt spinning,[12,26,27] no significant effect of the LCP on the high-order structure of the PET at low take-up velocities were found, while molecular orientation and orientation-induced crystallization were considerably suppressed at high velocities. X-ray studies of extruded sheets of PET, LCP, and their blends[12] showed a high degree of orientation along the extrusion direction. The orientation was mainly due to the crystallization rate of the

Correspondence to: R. E. S. Bretas (bretas@power.ufscar.br).

Contract grant sponsor: FAPESP and Brazilian Synchrotron Light Laboratory; contract grant number: D10A-XRD2-4254.

matrix, although adding LCP could also induce crystallization and orientation of the PET in the blends. Differential scanning calorimetry investigation of PET/LCP extruded strands[29,33] suggested that the LCP phase might act as a nucleating agent of the PET and that the orientation-induced crystallization of PET was accelerated by the presence of the LCP. In the case of stretched strands (at 80°C), the moduli increased with the stretching ratio due to the orientation-induced crystallization of PET. A large increase of the modulus was found in LCP-containing strands in the region of low (1–5) stretching ratio.[29]

Two techniques are known to be especially suitable for the study of molecular orientation in polymer systems: wide-angle X-ray scattering (WAXS) and polarized infrared spectroscopy (FTIR). The WAXS technique provides a very detailed picture of the bulk orientation distribution. Polarized FTIR, on the order hand, has been extensively used to investigate the surface orientation of many polymers.

X-ray pole figure analysis is an established technique for measuring the orientation distribution of crystallites, and hence their molecular constituents.[37–39] To describe the orientation of the crystallographic axes of the crystallites in a sample a three-dimensional coordinate system (machine, transverse and normal direction, MD, TD, and ND, respectively) is used. The orientation of a unit vector normal to a given crystallographic plane can then be described by two angles, χ and φ, where χ is the angle between MD and ND and φ is the angle between the projection of the normal to the ND/TD plane and TD. Pole figures provide a way to represent graphically the orientation distribution function of the normal to any selected crystallographic plane. Intensities for the complete X-ray pole figure contours are obtained by setting the position of the detector at a 2θ angle corresponding to a selected (hkl) reflection, while the sample assumes all possible orientations ($0 \leq \chi \leq 90^\circ$ and $0 \leq \varphi \leq 360^\circ$). The total peak intensity and the area under each deconvoluted peak must be used to correct the construction of the pole figures.

In this work, we have investigated the molecular orientation of the LCP phase in blends of PET with one rigid and one semi-flexible thermotropic LCP by WAXS pole figures. The blends films with various compositions were prepared by twin screw extrusion. The behavior of the uniaxial molecular orientation of the LCP phase as a function of composition and along the transverse section of the extruded films was reported. Moreover, the influence of a compatibilizer on the orientation parameter of both LCPs was also determined. Similar investigation by polarized infrared spectroscopy was the focus of the first part of this article.[13]

EXPERIMENTAL

Materials, blending, and film extrusion

The PET resin used was a copolymer based on terephthalic acid and ethylene glycol, kindly donated by Rhodia Ster of Brazil, known as RhoPET S80. The PET weight average molecular weight (M_w) was 30.000 g/mol and its melting temperature (T_m) was 235°C. Two thermotropic LCPs were used. One was a random copolyester of 75 mol % of poly(hydroxybenzoic acid) (HBA) and 25 mol % of poly(hydroxynaphthoic acid) (HNA), trade name Vectra®A950, supplied by Ticona, USA, with M_w and T_m of 30.000 g/mol and 280°C, respectively. The other LCP was made of 80 mol % HBA and 20 mol % poly(ethylene terephtalate), trade name Rodrun®LC5000, supplied by Unitika Co., Ltd. of Japan. The M_w and T_m were 20.000 g/mol and 280°C, respectively. The compatibilizer agent Lotader®AX8900 was used to enhance the interfacial interactions between the PET and the LCPs. This compatibilizer was supplied by Atofina of France and is a random terpolymer of 67 wt % of ethylene, 25 wt % of acrylic ester and 8 wt % of glycidyl methacrylate, with T_m of 60°C. All materials were dried in a vacuum oven at 150°C for 5 h prior to use. First a masterbatch of 80/20 LCP/compatibilizing agent was made by twin screw extrusion in a co-rotational ZSK30 Werner & Pfleiderer extruder. The films of the blends were subsequently produced in the same twin screw extruder, using a slit die and a set of rollers, where the films were uniaxially drawn at a constant draw rate of 6.32 m/min, cooled by air jet followed by immersion in water bath at 70°C. Films with compositions PET/LCP 95/5, 90/10, 85/15, and 0/100 and PET/LCP/compatibilizing agent 90/10/2.5, in wt % were thus produced with a width between 50 and 60 mm. Details of the processing conditions were already described in the literature.[13,36]

WAXS

The crystalline degree and the molecular orientation of the PET/LCPs films were characterized by WAXS measurements. Part of the WAXS measurements was carried out at the high-resolution X-ray diffraction beamline, D10A-XRD2, of the Brazilian Synchrotron Light Laboratory (LNLS), with a six-circle diffractometer with positive movement directions goniometer.[40] The beam energy was tuned to 6931.4 eV. The incident beam was collimated by a 3×1.6 mm diffraction slit coupled with a 0.5 mm slit located just before the detector. The other X-ray diffraction facility used was a Siemens diffractometer, model D5000, with Fe-filtered CoK_α radiation, operating at 33 kV and 50 mA. The incident beam was collimated by a 0.6-mm vertical diffraction slit coupled with a 0.6-mm horizontal divergent Schulz slit.

Diffractograms were obtained in the angle range between 10 and 70° using an interval of 0.05°. The crystallinity degree (X_C) of the samples was calculated as the ratio between the total area of the crystalline peaks (A_C) and the total area (crystalline peaks and amorphous halos) (A_a) of the diffractogram using eq. (1). The crystalline reflection and amorphous halos were fitted with Gaussian functions.

$$X_C\ (\%) = \frac{A_C}{A_C + A_a} \times 100 \quad (1)$$

The molecular orientation was characterized by WAXS pole figures. This data was obtained using a goniometer by rotating the films with scanning angle φ of $0 \leq \varphi \leq 360°$. Two experimental techniques were used to measure the intensities for a given Bragg angle θ: (i) the Schulz reflection method by tilting the sample from $0 \leq \chi \leq 65°$, where χ is the tilting angle; (ii) the Decker transmission method for the remaining χ values up to and including 90°.[37] An angle step of 5° for φ and χ was used during the measurements. Exposition times were adjusted in agreement with the intensities. The Siemens software did the data collection. The Polo2003 software performed correction of background, defocalisation and absorption effects and the connection between both experimental methods before the plotting of the pole figures. To quantify the *c*-axis LCP crystalline orientation along MD, the experimental pole figures were reconstructed by the Polo2003 software, which is based on spherical harmonics for texture analysis. This procedure is described in the literature.[37,38] From the measured diffracted intensities, the mean square cosine of the orientation angle Φ ($\langle \cos^2 \Phi_{hkl,MD} \rangle$) was calculated by the relation:

$$\langle \cos^2 \phi_{hkl,MD} \rangle = \frac{\int_0^{\pi} I(\phi) \sin \phi \cos^2 \phi \, d\phi}{\int_0^{\pi} I(\phi) \sin \phi \, d\phi} \quad (2)$$

where $\Phi_{hkl,MD}$ is the angle between the normal to the (hkl) crystalline plane and the direction of interest (MD). The quantity $\langle \cos^2 \Phi_{hkl,MD} \rangle$ is an average over all the crystallites in a sample.

The orientation of the *c*-axis (chain axis) relative to the MD was calculated by using the Hermans orientation factor ($f_{c,MD}$) given by eq. (3), in which *c* corresponds to the crystallographic chain axis. The orientation factor ranges from 0 for random orientation to 1 for perfect orientation or −1/2 for perpendicular orientation:

$$f_{c,MD} = \frac{3\langle \cos^2 \phi_{c,MD} \rangle - 1}{2} \quad (3)$$

The WAXS measurements were carried out at four different and equidistant positions located along the transverse (width) direction of the extruded films (from the center to the wall film),[13] as shown in Figure 1. The abbreviations c, nc, nw, and w mean: center, near of the center, near of the wall and at the wall of the film (5 mm from the film wall), respectively. The film average width was 50–60 mm.

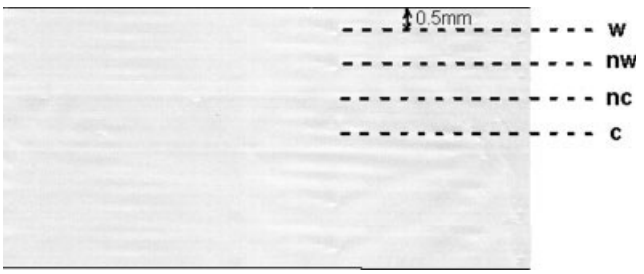

Figure 1 The four positions along the transverse direction of the blend extruded films where the molecular orientation was analyzed, where (w) at the wall; (nw) near the wall; (nc) near the center, and (c) center position.

RESULTS AND DISCUSSIONS

Figure 2 shows the X-ray diffractograms of both LCPs films obtained at room temperature. Both diffractograms show a strong peak at $2\theta = 51.0°$ corresponding to the (004) and (003) crystallographic planes. The molecular orientation of the chain axis in the crystalline region of both LCPs was evaluated by the analysis of the pole figures of the (00L) crystallographic plane. The normal to the (00L) plane is parallel to the *c*-axis. The normal to the (004) and (003) planes are the *c*-axis of the naphthalene and benzene rings of the LCP Vectra®A950 and Rodrun®LC5000, respectively.[16]

The X-ray pole figures of the (004) and (003) diffraction planes for both pure LCPs films are shown in Figures 3 and 4, respectively. These Figures show the pole figure resulting of the orientation measurements at all positions (c, nc, nw, and w) along the transverse direction of the extruded films. The pole figures were plotted in contour projections with the MD and transverse direction (TD) tilting 22.5° in the plane and the normal direction (ND) perpendicular to this plane. The maximum pole density is indicated by the isolines of the contour projection.

As can be observed in Figures 3 and 4, the pole figures showed characteristic forms of the (00L) crystallographic plane aligned parallel to the MD, indicating that the *c*-axis orientation of both pure LCPs is along the draw direction. From the pole density values, indicated by the isolines, it can be noted that both LCPs exhibit different orientation degree and that the *c*-axis orientation vary along the transverse section of the extruded films. $f_{c,MD}$ for both LCP films was calculated from the experimental (00L) pole figures using equations (2) and (3). Figure 5 shows $f_{c,MD}$ for the

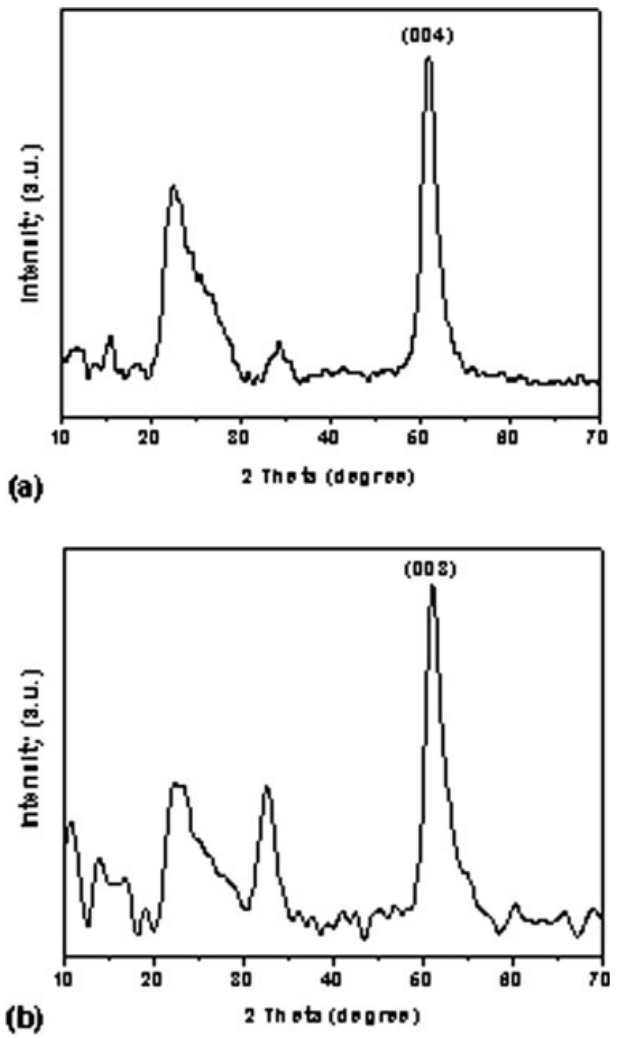

Figure 2 X-ray diffractogram of the pure LCP films (a) Vectra®A950 and (b) Rodrun®LC5000.

Vectra®A950 and Rodrun®LC5000 LCP films. In this Figure it is also shown the LCPs orientation along the transverse direction of the extruded films. Typical standard deviations of $f_{c,MD}$ values are approximately ± 0.05.

Regarding the molecular orientation along the transverse direction of the extruded pure LCPs films, it can be concluded that the chain axis orientation of both LCPs is parallel to the draw direction at all film positions. However, this orientation increases as the distance from the center of the films increases. At the w position (5 mm from the wall), this molecular orientation decreases again. At the center position the LCP orientation is almost null indicating random orientation of the LCP chains. The highest orientation effects are observed at the nw position. The LCP orientational behavior is due to the shear rate effects, which are minimum at the w position and maximum at the nw position.[13,41]

Systematic investigations about the effects of extensional flow and shear flow on the development of molecular orientation in thermotropic LCPs were evaluated by Ide et al.[42] and Viola et al.[43] It was found that extensional flow has a higher capacity of orientation in such materials than shear flow. Specifically extraordinary orientation is obtained with small elongation strains, but shear strain (or shear rate) has little effect. This finding was used to interpret the orientation distribution (skin-core morphology) of extruded and injection-molded articles.

Comparing the $f_{c,MD}$ values obtained for both LCPs, it is evident that the orientation degree of the Vectra®A950 is higher than of the Rodrun®LC5000 along the draw direction for films processed at the same conditions. This behavior was observed at all positions and is attributed to the stiffness difference between both LCPs, since the more rigid chains of the Vectra®A950 orient more effectively. Pan et al.[27]

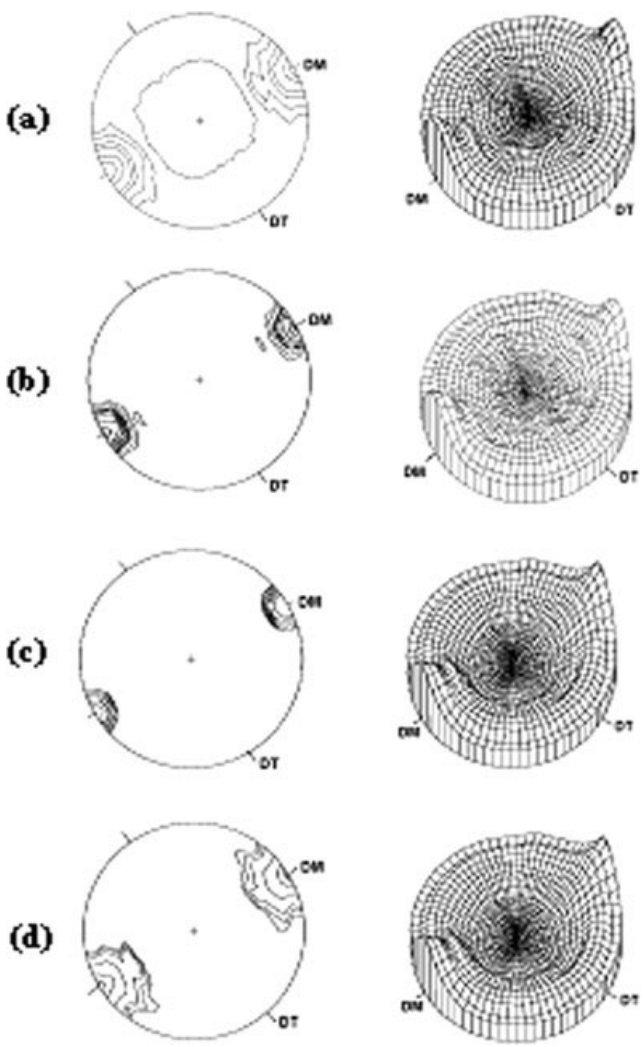

Figure 3 Contour and three-dimensional projections of X-ray pole figures of the (004) diffraction plane of pure Vectra LCP at the film positions: (a) c, (b) nc, (c) nw, and (d) w.

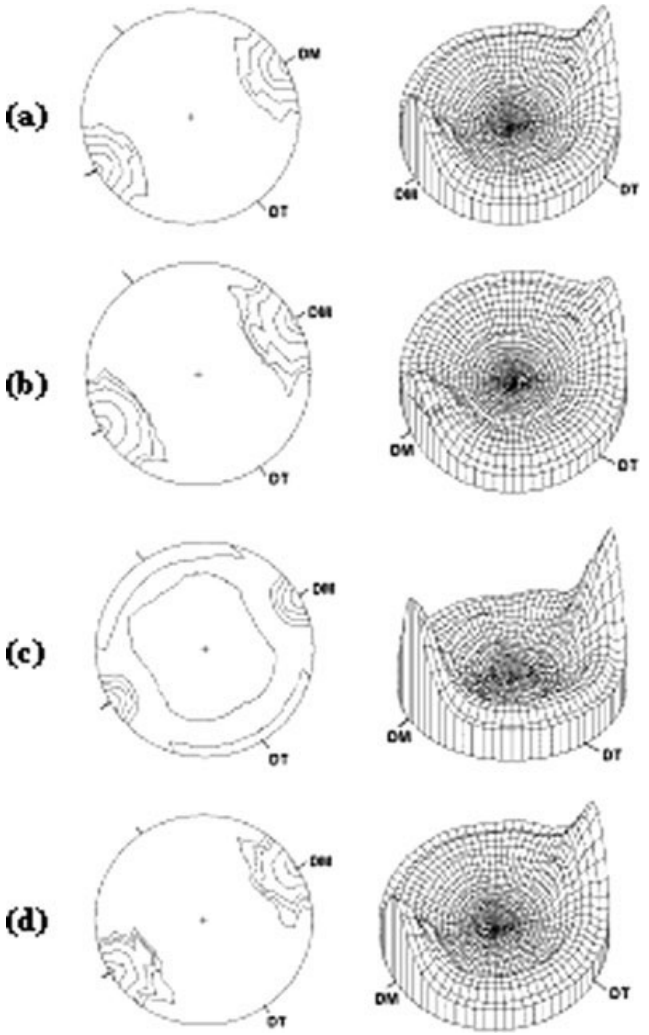

Figure 4 Contour and 3-dimensional projections of X-ray pole figures of the (003) diffraction plane of pure Rodrun LCP at the film positions: (a) c, (b) nc, (c) nw, and (d) w.

also observed by birefringence measurements that for blends of PET and two LCPs (60PHB-PET and VectraA900) obtained by melt spinning, the addition of the LCP with a less rigid chain produced a lower orientation of the as-spun fibers than the LCP with whole aromatic rigid chains.

The (004) and (003) X-ray pole figures of the PET/Vectra and PET/Rodrun blends measured for all compositions and at all four positions along the transverse direction of the extruded films are shown in Figure 6 and 7, respectively. The pole figures were plotted in contour projection. For better visualization and interpretation of the projection, the MD is the line running horizontally east to west, TD is the north to south vertical line and ND is the line perpendicular to the plane of the pole figure passing through the center of the pole. The maximum pole density is indicated by the isolines of the pole figures.

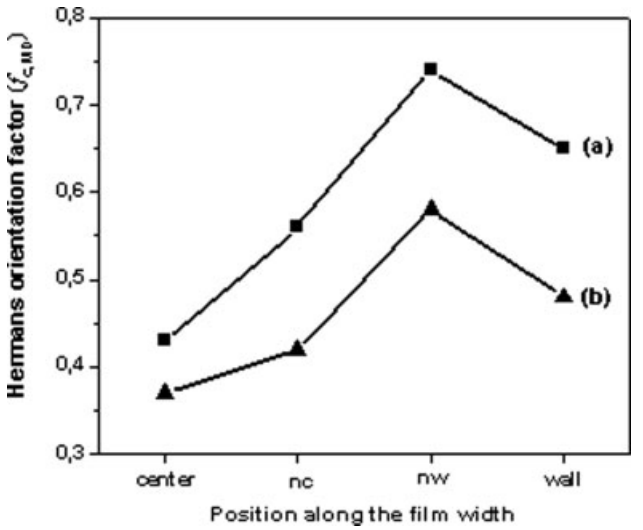

Figure 5 Hermans orientation factor in the MD ($f_{c,MD}$) and along the transverse section of the pure (a) Vectra and (b) Rodrun LCP films.

It is evident that both LCP molecules are also preferentially oriented in the draw direction. The pole figures show a maximum pole density in the machine direction. However, by looking at the magnitude of the pole density indicated by the isolines, it is clear that the orientation of the LCP molecules in the blends is very low in comparison with the orientation of both pure LCP films.

To obtain quantitative information about the effect of PET and of compatibilizer on both LCPs crystalline

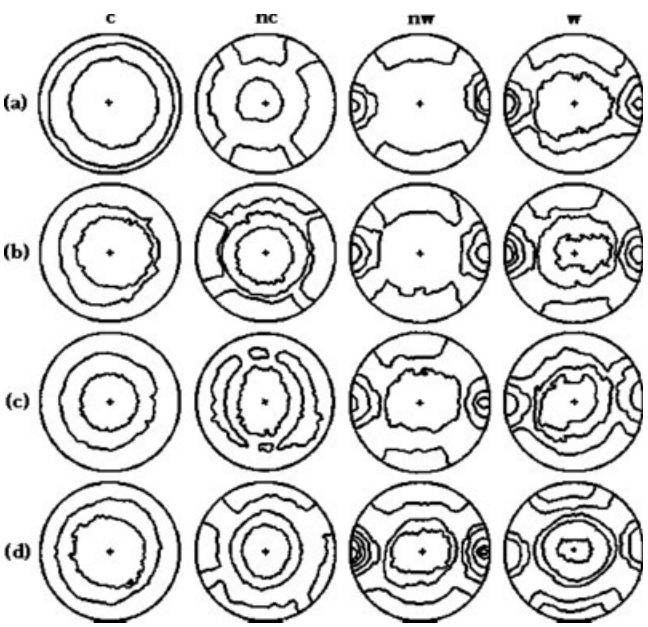

Figure 6 Contour plots X-ray pole figures for the (004) diffraction plane of the (a) 95/5, (b) 90/10, (c) 90/10/2.5, and (d) 85/15 PET/LCP Vectra blend films and at the film positions c, nc, nw, and w, respectively.

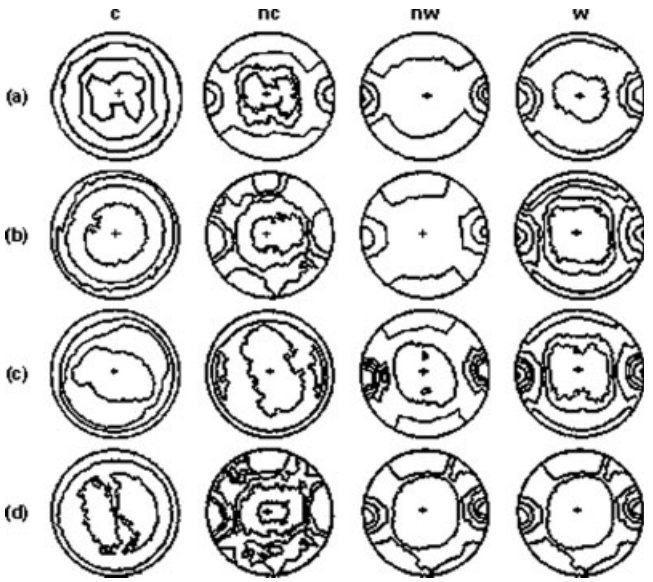

Figure 7 Contour plots of X-ray pole figures for the (003) diffraction plane of the (a) 95/5, (b) 90/10, (c) 90/10/2.5, and (d) 85/15 PET/LCP Rodrun blend films and at the film positions c, nc, nw and w, respectively.

orientation, Hermans orientation factors were calculated from the pole figure data. In Table I are listed the calculated $f_{c,MD}$ values for both blend systems; the *c*-axis crystalline molecular orientation of both LCP molecules, which vary as a function of the blend composition and along the transverse direction of the extruded films is also shown.

The $f_{c,MD}$ values revealed again preferential molecular orientation of both LCPs in the MD and also that the orientation in this direction is drastically lower in both blends than in the pure LCP films. Regarding the blends composition, it was observed a decrease in the LCPs molecular orientation with the decrease of the PET content in both PET/LCP blend systems.

Regarding the LCP chain molecular orientation along the transverse direction of the extruded blend films, the influence of the shear rate during the processing can be again observed, as for the pure LCP films. The calculated *c*-axis orientation factors (Table I) showed that the molecular orientation in the draw direction of both LCPs in the blends increased as the distance from the center of the films increased. At the position where the shear rate is minimum, c position, the LCP orientation was close to zero. At the nw position, the shear rate was maximum and therefore the LCP orientation was also maximum. However, at a distance of 5 mm from the wall, w position, the *c*-axis molecular orientation decreased again. The results also showed that in the blends the degree of the *c*-axis orientation of the Vectra®A950 molecules in the draw direction is higher than of the Rodrun®LC5000 molecules processed at the same conditions and at all film positions. All these

TABLE I
Average Hermans Orientation Factor ($f_{c,MD}$) of the LCP *c*-Axis in the Machine Direction and Crystallinity Degree (X_C) of PET/LCP Blends as a Function of the Composition and Along the Transverse Section of the Extruded Films

Blend PET/LCP	Pos.[a]	Vectra®A950		Rodrun®LC5000	
		$f_{c,MD}$	X_C (%)	$f_{c,MD}$	X_C (%)
100/0	c	–	9	–	9
	nc	–	11	–	11
	nw	–	13	–	13
	w	–	12	–	12
95/5	c	0.04	9	0.03	11
	nc	0.35	11	0.26	12
	nw	0.52	13	0.37	15
	w	0.45	12	0.32	13
90/10	c	0.03	10	0.02	11
	nc	0.32	11	0.24	11
	nw	0.46	14	0.35	15
	w	0.40	13	0.30	12
90/10/2.5[b]	c	0.02	10	0.03	12
	nc	0.30	12	0.22	13
	nw	0.43	14	0.31	14
	w	0.37	11	0.25	12
85/15	c	0.03	10	0.01	12
	nc	0.28	11	0.22	13
	nw	0.40	15	0.30	15
	w	0.37	13	0.26	14

[a] Positions along the transverse section of the extruded films; c, center position; nc, near the center; nw, near the wall; w, at the wall.
[b] Compatibilized blend.

behaviors can be analyzed by comparison of the $f_{c,MD}$ values of both LCPs listed in Table I, and by the pole figures (Figures 6 and 7).

The Herman factors of the compatibilized and noncompatibilized blends, calculated from the pole figures of Figures 6 and 7, are also shown in Table I; it is observed that the $f_{c,MD}$ values of the compatibilized blends are slightly lower than of the noncompatibilized blends. Therefore, the orientation of the compatibilized blends is lower than of the noncompatibilized ones. This lower orientation can be the result of a higher interaction between the components of the blends, which produces a reduction in the molecular motion of both LCPs in the draw direction. Comparing the two compatibilized blends, it is also observed that the $f_{c,MD}$ values of the Vectra®A950 blend are slightly higher than of the $f_{c,MD}$ values of the Rodrun®LC5000 blend at all positions, that is the interactions of the Rodrun with the compatibilizer are higher than the interactions between the Vectra and the compatibilizer. Tensile strength measurements on these films confirmed these results.[36]

In a previous study,[13] we reported the crystalline and amorphous molecular orientation of these polymers and their blends. The orientation was determined by FTIR and analyzed as a function of blend composition and along the transverse section of the extruded films. The effect of a compatibilizer agent was also evaluated. All results from the present work are in accordance with the orientation results made by the FTIR technique.

In the X-ray diffractograms of both blends, there was no distinct diffraction peaks for planes of the PET phase, therefore, it was not possible to characterize the molecular orientation of the PET phase. However, this characterization was systematically carried out by polarized FTIR and recently published.[13] The results showed that for the PET phase, an alignment of the amorphous phase in the draw direction due to the presence of the LCP and compatibilizer agent was obtained. The crystalline phase of PET, however, showed no significant orientation in the draw direction.

The cristallinity degree results along the transverse section of the extruded films are summarized in Table I. A low percentage of crystallinity, less than 13%, for the pure PET film at all positions was obtained. This crystallinity increased up to 15% when the LCP and compatibilizer were added. This result is in accordance with DSC results obtained by Silva[36] that also observed a crystallinity increase of $\sim$ 2% relative to the pure PET. Regarding the crystallinity degree along the transverse direction of the films no significant variation was found; however for both PET/LCP blend systems it can be observed that the crystallinity is maxima at the nw position and minimum at the c position.

CONCLUSIONS

Detailed qualitative and quantitative information regarding the uniaxial molecular orientation of the crystalline LCP in two PET/LCP blend systems was done by using pole figure analysis of WAXS data. The results showed that as a result of the processing conditions, the *c*-axis of both LCP molecules in the films showed high molecular orientation in the draw direction; however their orientation degree decreased drastically when blended with the PET. The orientation of the LCP decreased in the draw direction with the increase in LCP amount in the blends and increased as the distance from the center of the extruded films increased. The maximum orientation effect and the highest crystallinity degree in all blend compositions were observed at the position where the shear rate was the highest. A low increase of the crystallinity degree with increasing of LCP content in the blends was also observed. The compatibilizer agent reduced the orientation of both LCP molecules in both blend systems. The molecular orientation of the LCP was higher in the Vectra®A950 films than in the Rodrun®LC5000 films. Excellent correlation between the results of WAXS pole figures and polarized FTIR[13] was obtained.

The authors are grateful to Rhodia Ster of Brazil for the PET donation. Special thanks are given to Dr. G. Kellerman for the helpful WAXS experimental discussions.

References

1. La Mantia, F. P. Thermotropic Liquid Crystal Polymer Blends; Technomic Publishing: Lancaster, 1993.
2. Acierno, D.; La Mantia, F. P. Processing and Properties of Liquid Crystalline Polymers and LCP Based Blends; Chemtec Publishing: Ontario, 1993.
3. Moon, H. S.; Park, J. K.; Liu, J. H. J Appl Polym Sci 1996, 59, 489.
4. Chang, J. H.; Jo, B. W. J Appl Polym Sci 1996, 60, 939.
5. Eijndhoven-Rivera, M. J. V.; Wagner, N. J.; Hsiao, B. J Polym Sci Part B: Polym Phys 1998, 36, 1769.
6. Vallejo, F. J.; Eguiazábal, J. I.; Nazábal, J. Polymer 2000, 41, 6311.
7. Saengsuwan, S.; Mitchell, G. R.; Bualek-Limcharoen, S. Polymer 2003, 44, 5951.
8. Qi, K.; Nakayama K. J Mater Sci 2001, 36, 3207.
9. Kestenbach, H.-J.; Rogausch, K.-D. Mater Res 2002, 6, 75.
10. Saengsuwan, S.; Mitchell, G. R.; Bualek-Limcharoen, S. Polymer 2003, 44, 5951.
11. Bastida, S.; Eguiazábal, J. I.; Nazábal, J. Polymer 2001, 42, 1157.
12. Kojima, J.; Kikutani, T. Sen-i Gakkaishi 2005, 61, 29.
13. Branciforti, M. C.; Silva, L. B.; Bretas, R. E. S. J Appl Polym Sci 2006, 102, 2241.
14. Dutta, D.; Fruitwala, H.; Kohli, H.; Weiss, R. A. Polym Eng Sci 1990, 30, 1005.
15. Acierno, D.; Collyer, A. A. Rheology and Processing of Liquid Crystal Polymers; Chapman & Hall: London, 1996.
16. McLeod, M. A.; Baird, D. G. Polym Compos 1999, 20, 18.
17. Poli, G.; Paci, M.; Magagnini, P.; Scaffaro, R.; La Mantia, F. P. Polym Eng Sci 1996, 36, 1244.

18. Silva, L. B.; Ueki, M. M.; Farah, M.; Barroso, V. M. C.; Maia, J. M. L. P.; Bretas, R. E. S. Rheol Acta 2006, 45, 268.
19. Chiou, Y. P.; Chiou, K. C.; Chang, F. G. Polymer 1996, 37, 4099.
20. Miller, M. M.; Cowie, J. M. G.; Tait, J. G.; Brydon, D. L.; Mather, R. R. Polymer 1995, 36, 3107.
21. Holtsi-Miettinen, R. M.; Heino, M. T.; Sépala, J. V. J Appl Polym Sci 1995, 57, 573.
22. Miller, M. M.; Cowie, J. M. G.; Brydon, D. L.; Mather, R. R. Polymer 1997, 38, 1565.
23. Mehta, S.; Deopura, B. L. Polym Eng Sci 1993, 33, 931.
24. Petrovic, Z. C.; Farris, R. J Appl Polym Sci 1995, 58, 1077.
25. Petrovic, Z. C.; Farris, R. J Appl Polym Sci 1995, 58, 1349.
26. Liang, B.; Pan, L.; He, X. J Appl Polym Sci 1997, 66, 217.
27. Pan, L.; Liang, B. J Appl Polym Sci 1998, 70, 1035.
28. Song, C. H.; Isayev, A. I. Polymer 2001, 42, 2611.
29. Yoshikai, K.; Nakayama, K.; Kyotani, M. J Appl Polym Sci 1996, 62, 1331.
30. Mehta, S.; Deopura, B. L. J Appl Polym Sci 1995, 56, 169.
31. Mehta, S.; Deopura, B. L. Polym Bull 1991, 26, 571.
32. Turcott, E.; Nguyen, K. T.; Garcia-Rejon, A. Polym Eng Sci 2001, 41, 603.
33. Jin, Y.; Lan, Q.; Yu, Y.; Shi, W.; Bu, H. J Macromol Sci Part B Phys 2001, 40, 1003.
34. Radhakrishnan, J.; Kikutani, T.; Okui, N. Sen-i Gakkaishi 1996, 52, 618.
35. Grasser, W.; Schmidt, H.-W.; Giesa, R. Polymer 2001, 42, 8529.
36. Silva, L. B. PhD Thesis; Federal University of São Carlos: São Carlos, Brazil, 2003.
37. Alexander, L. E. X-Ray Diffraction Methods in Polymer Science; Wiley-Interscience: New York, 1969.
38. Cullity, B. D. Elements of X-Ray Diffraction. Hardcover, 1967.
39. Galeski, A.; Argon, A. S.; Cohen, R. E. Macromolecules 1991, 24, 3945.
40. Giles, C.; Yokaichiya, F.; Kycia, S. W.; Sampaio, L. C.; Ardiles-Saravia, D. C.; Franco, M. K. K.; Neuenschwander, R. T. J Synchrotron Rad 2003, 10, 430.
41. Bretas, R. E. S.; D'avila, M. A. Reologia de Polímeros Fundidos, 2nd ed.; EDUFSCar: São Carlos, Brazil, 2005.
42. Ide, Y.; Ophir, Z. Polym Eng Sci 1983, 23, 261.
43. Viola, G. G.; Baird, D. G.; Wilkes, G. L. Polym Eng Sci 1985, 25, 888.